Microscopic theory of surface diffusion

T. Ala-Nissila* and S. C. Ying
Department of Physics, Brown University, Providence, Rhode Island 02912
(Received 12 April 1990)

We develop a microscopic theory of surface diffusion of adatoms using the Mori continued-fraction formalism. Along the surface plane, the adatom motion is extended leading to diffusive behavior, while motion perpendicular to the plane is assumed bounded and oscillatory. In the high-friction limit, we find a novel analytic solution for the diffusion tensor in terms of generalized adiabatic potentials. We show how the inclusion of vertical motion can cause large quantitative changes in the values of the diffusion coefficients, while keeping the universal properties of surface diffusion in the high- and low-temperature limits qualitatively unaltered. We explicitly compute the diffusion tensor for a variety of different lattices and potentials. In the high-temperature limit, the theory recovers the diffusion of a Brownian particle in a viscous medium. In the low-temperature limit, we demonstrate how the Arrhenius form of activated diffusion and the geometric random-walk form of diffusion anisotropy arise from the theory.

I. INTRODUCTION

The classical diffusive motion of a particle in an external potential which is either random or periodic constitutes an important problem central to many different areas of physics.[1] Recently, analytic theory to the diffusive motion of a classical particle interacting with an inhomogeneous background has been developed by Ying.[2] In this approach, the various time-dependent correlation functions associated with the motion of a classical particle are expressed as a continued-fraction expansion via the Mori projection-operator formalism.[3] In the high-friction limit, it was found that the continued fraction could be truncated and an analytic expression obtained for the diffusion constant of a particle in a square lattice. For other more complicated symmetries, the diffusion tensor **D** can be calculated by inverting a matrix, which is infinite in terms of a set of reciprocal-lattice vectors.

This existing theory is formulated for the extended motion of a particle in all dimensions. When applied to surface kinetics, this implies that the motion of an adatom has to be treated as strictly two dimensional. This restriction has some shortcomings. First and foremost, by eliminating the vertical motion of the adatom, we lose the most readily observable normal vibrational mode of the adatom. Moreover, at a quantitative level, it has been shown that the coupling of the parallel motion to the vertical motion has also important consequence on the rate of diffusion.[4] Technically, the difficulty arises from the fact that, for a chemisorbed atom, the vertical motion is bounded and oscillatory in nature, while the motion parallel to the surface is extended. The extended basis function for describing the parallel motion is impractical for the description of the vertical motion.

The present paper has two main objectives. The first is to generalize the existing theory explicitly to the case of surface adatoms by including the case of vertical motion. In Sec. II, we outline the formalism for this more general case. A localized basis set is introduced for describing the spatial dependence of the adatom in the normal direction, as contrasted with the plane-wave basis used for the parallel extended motion. For calculation of the diffusion tensor, the inclusion of vertical motion eventually results in a renormalized friction and an effective adiabatic potential. In Sec. III we examine in some detail how **D** is influenced by the vertical motion for several different values of the coupling parameter connecting the vertical and parallel motions. More importantly, the present formalism facilitates future studies of the vibrational frequency of an adatom as relaxation of the mode involving motion perpendicular to the surface. This is often the most accessible mode in the experimental study of adatom vibrational excitations.

The second main objective is to focus in detail on the universal properties of classical surface diffusion, in particular, as regards the temperature dependence and anisotropy of **D**. The Arrhenius form of activated temperature dependence $D = D_0 e^{-\beta\Delta}$, where D_0 is a prefactor and Δ is a prefactor and Δ an energy barrier, is almost universally accepted and used in the interpretation of experimental data for surface diffusion.[5] For the anisotropy of the diffusion tensor, the simple geometric random-walk model is often evoked.[6,7] To date, most theoretical studies of these questions are based on molecular-dynamics simulations.[8-10] A highly successful approach to the numerical study of surface diffusion has concentrated in using dynamical corrections to the phenomenological transition-state theory (TST).[8,9,11] Simulations have shown that, at low temperatures, corrections to TST are small. The TST picture of diffusion, in which the particle performs series of uncorrelated, activated jumps across the classical saddle-point barrier, is then a good approximation of the true diffusion process. These simulations thus provide a justification for both the Arrhenius form, and a simple geometric random-walk picture of the an-

isotropy of **D**. However, as temperature increases, trajectories not included in the TST become important and one expects deviations from the random-walk picture. The present theory makes *no assumptions* about particular diffusion trajectories, but expresses the diffusion tensor in an inverse friction expansion. In the high-friction limit, we have studied in detail how the diffusion anisotropy changes as a function of temperature. In a previous work,[12] we have reported briefly how universal features such as the Arrhenius form, random-walk limit, and the high-temperature limit of Brownian motion arise as limiting cases of our theory. In Sec. III, we will examine these universal features in more detail for a variety of different symmetries and model potentials.

II. ANALYTIC THEORY OF SURFACE DIFFUSION

A. Basic Hamiltonian and variables

We start with a general Hamiltonian describing the adatom and substrate as

$$H=\frac{\mathbf{P}^2}{2M}+V(\mathbf{R},\{\mathbf{R}_l\})+H_s \ , \tag{2.1}$$

where

$$H_s=\sum_l \frac{\mathbf{P}_l^2}{2m}+W(\{\mathbf{R}_l\}) \ . \tag{2.2}$$

The first two terms in H describe the kinetic and potential energies of the adatom and its interaction with the substrate. The second part of the Hamiltonian H_s includes all the kinetic and potential energies of the substrate. For a classical adatom, the kinetic energy $P^2/2M$ factors out in a trivial manner and it is convenient to define a reduced Hamiltonian $H_r=H_s+V(\mathbf{R},\{\mathbf{R}_l\})$. We now introduce a projection operator $\mathcal{P}_b$. When operated on an arbitrary variable A, $\mathcal{P}_b$ corresponds to taking the partial thermal average over the background degrees of freedom, i.e.,

$$\mathcal{P}_b A=Z^{-1}\prod_l \int d\mathbf{P}_l \int d\mathbf{R}_l \, e^{-\beta H_r} A \ . \tag{2.3}$$

Here $Z=\prod_l \int d\mathbf{P}_l \int d\mathbf{R}_l \, e^{-\beta H_r}$. It is also useful to introduce an adiabatic potential $V_A(\mathbf{R})$ defined in the following way:

$$e^{-\beta V_A(\mathbf{R})}\equiv \mathcal{P}_b e^{-\beta V(\mathbf{R},\{\mathbf{R}_l\})} \ . \tag{2.4}$$

This adiabatic potential represents a potential experienced by the diffusing particle at point **R** averaged over the background vibrational degrees of freedom. Under normal conditions in the study of surface diffusion, the motion of the adatom perpendicular to the surface involves only small-amplitude oscillations. Denoting the coordinate vector parallel to the surface as **r** and the normal coordinates as z, we can expand the potential $V_A(\mathbf{r},z)$ around the local minimum $z_0(\mathbf{r})$ as

$$V_A(\mathbf{r},z)\approx V_1(\mathbf{r})+c[1+V_2(\mathbf{r})][z-z_0(\mathbf{r})]^2 \ .$$

Here $V_1(\mathbf{r})$ and $V_2(\mathbf{r})$ are periodic functions of **r** with the latter defined such that it contains only nonzero Fourier components. It is also convenient to change the variable from z to u so that

$$u\equiv(\beta c)^{1/2}[z-z_0(\mathbf{r})] \ .$$

In the following, we will set $\beta c=1$ for simplicty.

Next, we introduce a set of orthogonal variables $\{\mathbf{A}_n\}$ and their corresponding projection operators $\{\mathcal{P}_n\}$ of the diffusing particle:

$$\begin{aligned}
&\mathbf{A}_0=[e^{i\mathbf{G}\cdot\mathbf{r}}\psi_j(u)] \ , \\
&\mathbf{A}_1=\left[\frac{\mathbf{P}}{M}e^{i\mathbf{G}\cdot\mathbf{r}}\psi_j(u)\right] \ , \\
&\cdots \ , \\
&\mathbf{A}_n=(1-\mathcal{P}_{n-1}-\mathcal{P}_{n-2})\mathcal{P}_b\,\mathbf{A}_{n-1} \ .
\end{aligned} \tag{2.5}$$

Here, the **G**'s stand for the set of two-dimensional reciprocal-lattice vectors appropriate for the substrate, and

$$\psi_j(u)=\frac{1}{(2^j\pi^{1/2}j!)^{1/2}}H_j(u)$$

are eigenfunctions proportional to the jth-order Hermite polynomials which have been normalized such that

$$\int_{-\infty}^{+\infty} du \ \psi_j(u)\psi_{j'}(u)e^{-u^2}=\delta_{jj'} \ .$$

Note that, in our definition, each basic variable $\mathbf{A}_n$ has actually an infinite number of components corresponding to different reciprocal-lattice wave vectors, Cartesian coordinates of the momentum vector, and the order of the functions ψ_j. In (2.5), the projection operators are defined as

$$\mathcal{P}_n\,\mathbf{A}=\mathbf{A}\chi_{nn}^{-1}(\mathbf{A}_n,\mathbf{A}) \tag{2.6}$$

with

$$\chi_{nn}=(\mathbf{A}_n,\mathbf{A}_n) \ ,$$

where the scalar product (A,B) is defined as the thermal average of A^*B. It is easy to verify from these definitions that the **A**'s are orthogonal to each other. With these definitions of the basic variables and the projection operators we can now apply the standard Mori formalism[3] to obtain a formal equation for the Laplace transform of the correlation functions $\boldsymbol{\phi}_{nn'}(\omega)$ defined as

$$\phi_{nn'}(\omega)=\int_0^\infty e^{i\omega t}\boldsymbol{\phi}_{nn'}(t)\,dt \ . \tag{2.7}$$

The resulting equation for $\boldsymbol{\phi}(\omega)$ is

$$[-i\omega\chi^{-1}+\mathbf{b}+\boldsymbol{\Sigma}(\omega)]\boldsymbol{\phi}(\omega)=\mathbf{1} \tag{2.8}$$

with

$$\mathbf{b}=i\chi^{-1}(\mathbf{A},L\,\mathbf{A})\chi^{-1}$$

and

$$\boldsymbol{\Sigma}(\omega)=\chi^{-1}\left[QL\,\mathbf{A},\frac{i}{\omega-QLQ}QL\,\mathbf{A}\right]\chi^{-1} \ .$$

In this equation, Q is the projection operator into the space orthogonal to that spanned by the basic variables $\{\mathbf{A}_n\}$,

$$Q=1-\sum_{i=0}^{\infty}\mathcal{P}_i \tag{2.9}$$

and L is the Liouville operator.

The set of equations in (2.8) is equivalent to the Kramer's equation.[2] However, since we start from a lattice dynamic Hamiltonian, there is an additional bonus here in the fact that, instead of a phenomenological damping constant, we have a memory function $\Sigma(\omega)$ which contains the damping effects. As we shall see in the next section, the memory function can be related to the vibrational properties of the background.

B. Inverse friction expansion

Starting from the general equation (2.8) for the correlation functions $\phi_{nn'}(\omega)$, we can develop a continued-fraction expansion for $\phi_{11}(\omega)$ which is directly related to the diffusion constant. As we shall see below, this expansion is actually an expansion in inverse powers of the friction. The leading term corresponding to the high-friction limit has a very simple form. Let us define

$$\mathbf{a}_i(\omega)\equiv -i\omega\chi_{ii}^{-1}+\Sigma_{ii}(\omega)\ . \tag{2.10}$$

Then, from (2.8), we obtain the set of equations

$$\begin{aligned}
&\mathbf{a}_0\boldsymbol{\phi}_{01}(\omega)+\mathbf{b}_{01}\boldsymbol{\phi}_{11}(\omega)=\mathbf{0}\ ,\\
&\mathbf{b}_{10}\boldsymbol{\phi}_{01}(\omega)+\mathbf{a}_1\boldsymbol{\phi}_{11}(\omega)+\mathbf{b}_{12}\boldsymbol{\phi}_{21}(\omega)=\mathbf{1}\ ,\\
&\ldots\ ,\\
&\mathbf{b}_{n,n-1}\boldsymbol{\phi}_{n-1,1}(\omega)+\mathbf{a}_n\boldsymbol{\phi}_{n1}(\omega)+\mathbf{b}_{n,n+1}\boldsymbol{\phi}_{n+1,1}(\omega)=0\\
&\qquad\qquad\qquad\qquad\qquad\qquad\text{for } n>1\ .
\end{aligned} \tag{2.11}$$

Now we introduce the functions $\mathbf{B}_n(\omega)$ defined as

$$\boldsymbol{\phi}_{n1}(\omega)=\mathbf{B}_{n-1}(\omega)\boldsymbol{\phi}_{n-1,1}(\omega)\ . \tag{2.12}$$

Then we have from (2.10)

$$\boldsymbol{\phi}_{11}(\omega)=[\mathbf{a}_1-\mathbf{b}_{10}\mathbf{a}_0^{-1}\mathbf{b}_{01}+\mathbf{b}_{12}\mathbf{B}_1(\omega)]^{-1} \tag{2.13}$$

and for $n>1$

$$\mathbf{B}_{n-1}(\omega)=-[\mathbf{a}_n+\mathbf{b}_{n,n+1}\mathbf{B}_n(\omega)]^{-1}\mathbf{b}_{n,n-1}\ . \tag{2.14}$$

Equations (2.13) and (2.14) together constitute a continued-fraction expansion for the correlation function $\boldsymbol{\phi}_{11}(\omega)$. Note that the diffusion tensor, which is the zero-frequency limit of the Laplace transform of the velocity autocorrelations function,[3] is given in terms of $\boldsymbol{\phi}_{11}(\omega)$ by the expression

$$\begin{aligned}
D_{\alpha\beta}&=\int_0^{\infty}\langle V_\alpha(t)V_\beta(0)\rangle dt\\
&=\lim_{\omega\to 0}[\boldsymbol{\phi}_{11}^{\alpha\beta}(\mathbf{G}=0,j=0;\mathbf{G}'=0,j'=0;\omega)]\ .
\end{aligned} \tag{2.15}$$

In the limit $\omega\to 0$, the a's are proportional to the friction memory function $\Sigma_{ii}(\omega)$. Therefore, the continued-fraction expansion (2.13) and (2.14) is equivalent to an inverse friction expansion. In the high-friction limit, we can drop all the $\mathbf{B}_n(\omega)$ in the continued-fraction expansion for $n>1$, the result for $\boldsymbol{\phi}_{11}(\omega)$ is then the simple expression

$$\boldsymbol{\phi}_{11}(\omega)=[\mathbf{a}_1(\omega)-\mathbf{b}_{10}\mathbf{a}_0^{-1}(\omega)\mathbf{b}_{01}]^{-1}\ . \tag{2.16}$$

Equation (2.16) is a formal solution in the high-fraction limit and so it is equivalent to a solution of the corresponding Smoluchowski equation.[2] The important feature of the present method is that we also have a microscopic expression for the frictional force. Equation (2.16) can be simplified further. First, we note that

$$\chi_{11}=\frac{k_BT}{M}\chi_{00}\delta_{\alpha\beta}\ , \tag{2.17}$$

and hence

$$\mathbf{a}_1(\omega)=-i\omega\frac{M}{k_BT}\delta_{\alpha\beta}\chi_{00}^{-1}+\Sigma_{11}(\omega)\ . \tag{2.18}$$

Next, we show in the Appendix that the matrix elements of

$$\mathbf{F}(\omega)\equiv\mathbf{b}_{10}\mathbf{a}_0^{-1}(\omega)\mathbf{b}_{01}$$

appearing in (2.16) are given by

$$\begin{aligned}
\mathbf{F}^{\alpha\beta}(s,s';\omega)&=\frac{-i}{\omega}G_\alpha\chi_{00}^{-1}(\mathbf{G},\mathbf{G}';j,j')G'_\beta\ ,\\
\mathbf{F}^{zz}(s,s';\omega)&=-\frac{2i}{\omega}[(j+1)(j'+1)]^{1/2}\\
&\quad\times\chi_{00}^{-1}(\mathbf{G},\mathbf{G}';j+1,j'+1)\ ,\\
\mathbf{F}^{\alpha z}(s,s';\omega)&=\frac{[2(j'+1)]^{1/2}}{\omega}G_\alpha\chi_{00}^{-1}(\mathbf{G},\mathbf{G}';j,j'+1)\ ,\\
\mathbf{F}^{z\alpha}(s,s';\omega)&=\frac{\sqrt{2(j+1)}}{\omega}G'_\alpha\chi_{00}^{-1}(\mathbf{G},\mathbf{G}';j+1,j')\ ,
\end{aligned} \tag{2.19}$$

for $\alpha,\beta=x,y$. Here $s\equiv(\mathbf{G},j)$, and we have listed the indices in χ_{00}^{-1} in detail. In terms of $\mathbf{F}$, we finally have the general result for the frequency-dependent velocity-velocity correlation function:

$$\boldsymbol{\phi}_{11}(\omega)=\left[-i\omega\frac{M}{k_BT}\delta_{\alpha\beta}\chi_{00}^{-1}+\Sigma_{11}(\omega)+\mathbf{F}(\omega)\right]^{-1}\ . \tag{2.20}$$

C. Density and the memory function

The two fundamental matrices needed in the evaluation of $\boldsymbol{\phi}_{11}(\omega)$ through Eq. (2.20) are χ_{00}^{-1} and $\Sigma_{11}(\omega)$. We shall show here how they are related to the density of the adatom and the substrate vibrational properties. First, it is easy to see from the definition of χ_{00} and the adiabatic potential $V_A(\mathbf{R})$ in (2.4) that

$$\chi_{00}(s,s')=\int d\mathbf{r}\int du\ n(\mathbf{r},u)\psi_j(u)\psi_{j'}(u)e^{-i(\mathbf{G}-\mathbf{G}')\cdot\mathbf{r}}\ . \tag{2.21}$$

Here $n(\mathbf{r},u)=Z^{-1}e^{-\beta V_A(\mathbf{r},u)}$ [$\beta=(k_BT)^{-1}$ and $Z=\int d\mathbf{r}\int du\ e^{-\beta V_A}$] is just the average density of the adatom. However, since

$$V_A(\mathbf{r},u)=V_1(\mathbf{r})+k_BT[1+V_2(\mathbf{r})]u^2 , \tag{2.22}$$

the density function $n(\mathbf{r},u)$ can be simplified to

$$n(\mathbf{r},u)=\tilde{n}(\mathbf{r},u)e^{-u^2} , \tag{2.23}$$

with

$$\tilde{n}(\mathbf{r},u)=Z^{-1}e^{-\beta[V_1(\mathbf{r})+V_2(\mathbf{r})\beta^{-1}u^2]}e^{-u^2}$$

being the reduced density. Note that the boundary condition that the motion is bounded in the z direction imposes the restriction $V_2(\mathbf{r})<1$. Substitution of (2.23) into (2.21) results in the following expression for χ_{00}:

$$\chi_{00}(s,s')=\int d\mathbf{r}\int du\ \tilde{n}(\mathbf{r},u)\psi_j(u)\psi_{j'}(u)e^{-u^2}e^{-i(\mathbf{G}-\mathbf{G}')\cdot\mathbf{r}} . \tag{2.24}$$

From (2.24), we can easily accomplish the inversion of the matrix χ_{00} to obtain

$$\chi_{00}^{-1}(s,s')=\frac{1}{A_0^2}\int d\mathbf{r}\int du\ \tilde{n}^{-1}(\mathbf{r},u)\psi_j(u)\psi_{j'}(u)\times e^{-u^2}e^{-i(\mathbf{G}-\mathbf{G}')\cdot\mathbf{r}} . \tag{2.25}$$

In (2.25), the integration $d\mathbf{r}$ is over the unit cell with area A_0.

The memory function contains the details of the coupling of the adatom motion to the background vibration. Here we examine the most important component—the (1,1) element of the memory function Σ in detail. From (2.8) we have

$$\Sigma_{11}(\omega)=\frac{k_BT}{M}\chi_{11}^{-1}\gamma(\omega)\chi_{11}^{-1} \tag{2.26}$$

with

$$\gamma(\omega)=\frac{1}{Mk_BT}\int_0^\infty dt\ e^{i\omega t}(QL\mathbf{P}\mathbf{A}_0,e^{-iQLQt}QL\mathbf{P}\mathbf{A}_0) . \tag{2.27}$$

It is easy to see that, to lowest order in the displacement of the substrate atoms, we have

$$QL\mathbf{P}\mathbf{A}_0=-(1-\mathcal{P}_b)\frac{\partial V}{\partial\mathbf{R}}e^{i\mathbf{G}\cdot\mathbf{r}}\psi_j(u) . \tag{2.28}$$

The $\mathbf{G}=0$, $j=0$ component of (2.28) corresponds simply to the frictional force on the atom due to the vibrational motion of the substrate. The projection operator Q serves to separate out the regular force on the adatom due to the interaction with the substrate at the equilibrium position $\{\mathbf{R}_l^0\}$. There is one limiting case when γ can be simplified considerably. This is when the time scale of the diffusive motion is much longer than the time scale for the vibrational motion of the background. Under this circumstance, the time dependence of the coordinates of the diffusing particle can be neglected in the memory function and replaced by its initial value. This is the initial value approximation.[13] In this approximation, γ decouples into the product of averages involving the adatom and the substrate atoms separately.

To simplify the memory function further, we now consider the case of a pairwise interaction potential, and utilize the harmonic approximation for the background vibrational motion. In this case the adiabatic potential $V_A(\mathbf{R})$ is given by the expression

$$V_A(\mathbf{R})=\sum_l v^{\text{eff}}(\mathbf{R}-\mathbf{R}_l) , \tag{2.29}$$

where v^{eff} is the thermally averaged pair interaction of the adatom with the substrate atom at position $\mathbf{R}_l$. The expression for γ can then be simplified to

$$\gamma^{\alpha\beta}(\omega)=\int d\mathbf{r}\int du\ \tilde{n}(\mathbf{r},u)\psi_j(u)\psi_{j'}(u)\eta^{\alpha\beta}(\mathbf{r},u;\omega)\times e^{-u^2}e^{-i(\mathbf{G}-\mathbf{G}')\cdot\mathbf{r}} , \tag{2.30}$$

where

$$\eta^{\alpha\beta}(\mathbf{r},u;\omega)=\frac{1}{Mk_BT}\sum_{l,l';\gamma,\delta}C_{ll'}^{\gamma\delta}(\omega)v_{\text{eff}}^{\alpha\gamma}(\mathbf{R}-\mathbf{R}_l^0)\times v_{\text{eff}}^{\beta\delta}(\mathbf{R}-\mathbf{R}_{l'}^0) . \tag{2.31}$$

In (2.31),

$$C_{ll'}^{\gamma\delta}(\omega)=\int_0^\infty dt\ e^{i\omega t}(u_{l\gamma},e^{-iQLQt}u_{l'\delta}) \tag{2.32}$$

and $\mathbf{R}=(\mathbf{r},z)$. The variable $u_{l\alpha}$ denotes a spatial α component of the lattice displacement at site l. The time dependence of the substrate correlation function in (2.32) is still governed by the complicated Liouville operator QLQ. In the weak-coupling approximation, we can neglect the influence of the diffusing particle on the vibrational motion of the background. This amounts to replacing the operator QLQ by the simpler operator L describing the dynamics of the substrate alone. Substitution of (2.27) into (2.26) and using (2.17) and (2.25) finally yields the expression for Σ_{11} as

$$\Sigma_{11}^{\alpha\beta}(s,s';\omega)=\frac{M}{A_0^2k_BT}\int d\mathbf{r}\int du\ \tilde{n}^{-1}(\mathbf{r},u)\eta^{\alpha\beta}(\mathbf{r},u;\omega)\psi_j(u)\psi_{j'}(u)e^{-u^2}e^{-i(\mathbf{G}-\mathbf{G}')\cdot\mathbf{r}}$$

$$=\frac{M}{A_0^2k_BT}\int d\mathbf{r}\int du\ \tilde{\eta}^{\alpha\beta}(\mathbf{r},u;\omega)\psi_j(u)\psi_{j'}(u)e^{-u^2}e^{-i(\mathbf{G}-\mathbf{G}')\cdot\mathbf{r}} . \tag{2.33}$$

D. Analytic solution for special symmetries

To solve for the diffusion tensor in the most general case, one has to use Eq. (2.20) and invert the matrix on the right-hand side numerically for a given finite set of reciprocal-lattice vectors and Hermite polynomials, and verify convergence. However, for the special case of lattices with square or simple rectangular symmetry, it is possible to achieve the inversion analytically in a closed form. Denoting the set of **G** vectors for these lattices as

$$\{\mathbf{G}_{nm}\}=\left\{\left[\frac{2\pi n}{a_x},\frac{2\pi m}{a_y}\right]\right\}, \tag{2.34}$$

where a_x and a_y are the lattice constants, it follows immediately that the diagonal elements of the diffusion tensor are given by

$$\begin{aligned} D_{xx}&=[\Sigma_{11}^{xx}(G_y,G_y';j,j';\omega=0)]^{-1}|_{G_y=G_y'=0;j=j'=0}\,,\\ D_{yy}&=[\Sigma_{11}^{yy}(G_x,G_x';j,j';\omega=0)]^{-1}|_{G_x=G_x'=0;j=j'=0}\,,\\ D_{zz}&=0\,. \end{aligned} \tag{2.35}$$

Using the simplified initial value form of the memory function, its inverse can easily be found and (2.35) leads to the following result:

$$D_{\alpha\alpha}=\frac{a_\alpha^2 k_B T}{M}Z^{-1}\int dx_\beta\int_{-\infty}^{+\infty}du\frac{e^{-u^2}}{\sqrt{\pi}}\left[\int dx_\alpha\, e^{V_1(\mathbf{r})/k_BT}e^{V_2(\mathbf{r})u^2}\eta^{\alpha\alpha}(\mathbf{r},u;\omega=0)\right]^{-1}, \tag{2.36}$$

where α and β refer either to the x or y direction, and x_α,x_β denote x,y or y,x.

Integrals of x and y in (2.36) are over the unit cell with area $A_0=a_xa_y$. For the square lattice case, D is fully isotropic and the order of the spatial integration variables in (2.36) does not matter. In the limit where the coupling constant $c\to\infty$, and $V_2\to 0$, $e^{-u^2}/\sqrt{\pi}$ is proportional to $\delta[z-z_0(\mathbf{r})]$. The formula (2.36) then reduces to the same form as the earlier two-dimensional result by Ying.[2] We note that the zero-frequency diffusion constant D_{zz} always vanishes, as the motion in the vertical direction is bounded.

III. DIFFUSION ON SURFACES WITH DIFFERENT SYMMETRIES

In this section we shall apply the microscopic theory of Sec. II to study diffusion in a variety of two-dimensional lattices. To this end, we will consider model systems and compute **D** as a function of temperature. In these systems, both the adiabatic potential $V_A(\mathbf{R})$ and the friction tensor $\eta^{\alpha\beta}(\mathbf{R};\omega=0)$ are chosen to be simple functions which nevertheless correctly obey the underlying symmetry of the lattice. On a square lattice, our simple analytic formula Eq. (2.36) allows us to study the effect of the bounded vertical oscillations on diffusion. For lattices with more complicated symmetries, we compute **D** using (2.20). In this work, we shall concentrate on such fundamental questions as the validity and emergence of the Arrhenius form of activated diffusion and the random-walk limit of diffusion, and the role of multiple, physically distinct, saddle points in determining diffusion anisotropies.

A. The square lattice

For a square lattice, the analytic formula (2.36) reduces to an isotropic form. As we have shown earlier,[12] in the low-temperature limit, the Arrhenius form $D=D_0e^{-\beta\Delta}$ follows, where D_0 is a prefactor and Δ is the difference between the saddle point and the minimum of V_A. In the opposite high-temperature limit, (2.36) recovers the isotropic form of diffusion of a Brownian particle in a viscous medium, with $D=(k_BT)/M\eta'$, where η' is a renormalized friction. Thus, the microscopic theory correctly incorporates the universal features of diffusion at all temperatures.

To study the effect of the vertical motion to diffusion, we will next consider the following simple forms for the potentials V_1 and V_2, as discussed in (2.22) of Sec. II:

$$\begin{aligned} V_1(\mathbf{r})&=V_0[\cos(\mathbf{G}_{10}\cdot\mathbf{r})+\cos(\mathbf{G}_{01}\cdot\mathbf{r})]\,,\\ V_2(\mathbf{r})&=V_0'[\cos(\mathbf{G}_{10}\cdot\mathbf{r})+\cos(\mathbf{G}_{01}\cdot\mathbf{r})]\,, \end{aligned} \tag{3.1}$$

where we vary the ratio V_0'/V_0. For the case where $V_0'\equiv 0$, we get the exact result

$$D=\frac{1}{\beta M\eta}[I_0(\beta V_0)]^{-2} \tag{3.2}$$

assuming a constant, isotropic friction tensor. Equation (3.2), in which I_0 denotes the hyperbolic Bessel function of order zero, is a generalization of the corresponding one-dimensional solution. In Fig. 1 we show this solution for $V_0=\frac{1}{2}$. When $V_0'>0$, we have to integrate (2.36) numerically. In Fig. 1 we further display results for two cases, for which V_0'/V_0 is $\frac{1}{2}$ and $\frac{9}{10}$. When the ratio approaches unity, the effect of the vertical oscillations become quantitatively rather large. First, the friction in the

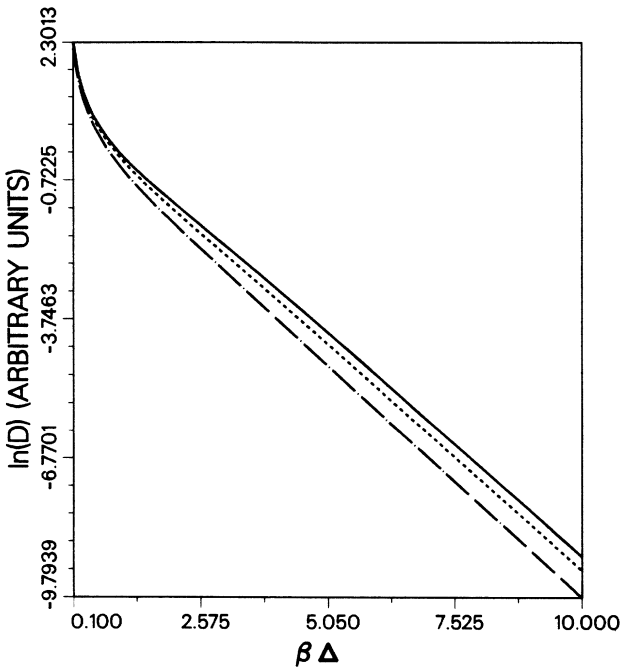

FIG. 1. Effect of the coupling of the vertical motion to diffusion on a square lattice. Upper solid line indicates the exact solution given by (3.2) without vertical motion, while the two other curves are for $V_0'/V_0=\frac{1}{2}$ (dashed line) and $\frac{9}{10}$ (dash-dotted line).

Brownian form of uniform diffusion is renormalized by V_2. Also, at intermediate temperatures, a finite V_2 changes the effective diffusion barrier. In the low-temperature limit, the barrier will be determined by V_1 alone; however, the prefactor D_0 decreases with increasing V_0', leading to reduced diffusion rates. For example, at $\beta\Delta=10$, D for $V_0'=0$ is about a factor 2.4 larger than for $V_0'/V_0=\frac{9}{10}$. Thus, we can conclude that bounded vertical motion can cause substantial quantitative changes in D. On the other hand, the *universal* features exhibited by the theory in the limits of very small or large temperatures compared to the effective barrier, remain qualitatively unchanged.

B. The centered rectangular lattice

For a lattice for which the set of lattice vectors $\{\mathbf{R}_l^0\}$ forms a centered rectangular lattice, the analytic solution (2.36) is no longer valid. To solve for $\mathbf{D}$, we have to calculate the matrix elements of χ_{00}^{-1}, Σ_{11}, and $\mathbf{F}$, and find the inverse of the right-hand side of (2.20). As we have seen in the previous section, the universal properties of diffusion are unaltered by the oscillatory vertical motion. Thus, in this and in the following sections we will set $V_2\equiv 0$ which will not change the qualitative features of our results. Consequently, we consider the case for which the matrix index s contains only reciprocal-lattice vectors, i.e., $s=(\mathbf{G},j=0)$, and the convergence of the results is determined by the number N of $\mathbf{G}$ vectors kept. As the temperature decreases, the corrugation in the density increases, and the value of N required for convergence is correspondingly larger. Typically, N must be of the order of 300–400 for the lowest-temperature results presented below.

To incorporate temperature-dependent substrate effects into the calculation of surface diffusion, we have to examine the temperature dependence of the friction tensor η. From the continuum theory of lattice vibrations, we can see that the factor $\beta C_{ll'}^{\gamma\delta}$ in the friction tensor (2.31) is independent of temperature.[14] Within this approximation, the main temperature dependence left then comes from the Debye-Waller correction factor in the effective potential $v_{\text{eff}}(\mathbf{R}-\mathbf{R}_l^0)$.[13] Within the harmonic approximation, this factor can be written as[15]

$$d_w=e^{-w}\ , \tag{3.3}$$

where

$$w(\mathbf{G}_i)=\frac{3h^2T^2}{8\pi^2Mk_B\theta_D^3}|\mathbf{G}_i|^2\int_0^{\theta_D/T}dx\frac{xe^x}{e^x-1}\ , \tag{3.4}$$

for each reciprocal-lattice vector $\mathbf{G}_i$ using standard Debye theory. Here θ_D is the Debye temperature of a given substrate. In the spirit of our model calculations, we will simply use expression (3.3) and multiply each Fourier component of the adiabatic potential and the friction tensor by d_w and d_w^2, respectively.

In Fig. 2 we show the general geometry pertaining to the centered rectangular lattice. The simplest periodic, effective potential can be written down as

$$V_1(\mathbf{r})=V_0[\cos(\mathbf{G}_1\cdot\mathbf{r})+\cos(\mathbf{G}_2\cdot\mathbf{r})]\ ,$$

with

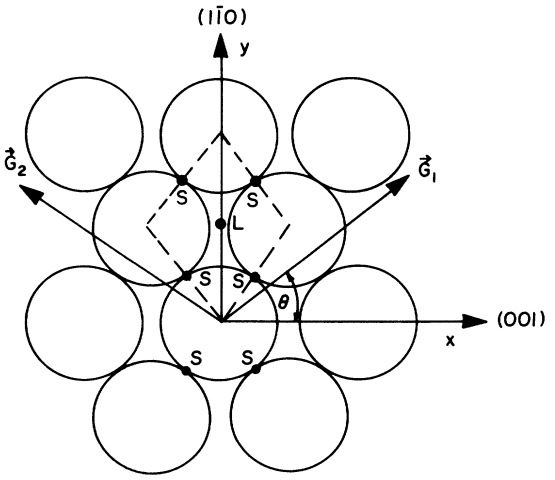

FIG. 2. Geometry of the rhomboidal lattice used in diffusion calculations. For the case of a W(110) lattice with centered rectangular symmetry, $\cot\theta=\sqrt{2}$. The adiabatic potentials are chosen such that the long bridge sites L correspond to potential minimum, while classical saddle points are located at short bridge sites S. $\mathbf{G}_1$ and $\mathbf{G}_2$ denote the two basic reciprocal-lattice vectors.

$$\mathbf{G}_1=(\cos\theta,\sin\theta)G_0 ,$$

$$\mathbf{G}_2=(-\cos\theta,\sin\theta)G_0 ,$$

and

$$G_0=\pi/(a\cos\theta\sin\theta) ,$$

where a is the separation between nearest-neighbor atoms. The choice of axes in Fig. 2 corresponds to the principal axes of diffusion, in which $\mathbf{D}$ is diagonal. The adiabatic potential possesses identical saddle points located at the short bridge sites S between atoms, while the minima are at the long bridge sites L. This geometry is believed to describe the diffusion of oxygen adatoms on W(110) surface, which has been studied both experimentally and theoretically.[6,7] For this surface, $\cot\theta=\sqrt{2}$.

In Fig. 3, we show results of our numerical calculations for a simple choice of the friction tensor, namely $\eta^{xx}=\eta^{yy}=1$, $\eta^{xy}=\eta^{yx}=0$. To include the Debye-Waller factors, we have used (3.4) and set $\theta_D=240$ K and $\Delta=1$ eV. This choice, in which the Debye temperature corresponds to the known value for the W(100) surface,[16] and for which the barrier is very large, produces relatively large Debye-Waller correction factors at higher temperatures. Even with these parameters, the effect of this correction is rather small for $\beta\Delta>5$, compared to our calculations with $d_w\equiv 1$.

In the high-temperature limit, the solution depicted in Fig. 3 correctly captures the isotropic limit of a Brownian particle. At low temperatures, both D_{yy} and D_{xx} cross over to an Arrhenius form at about $\beta\Delta\sim 5$, which correctly includes the energy barrier Δ as given by the difference between the saddle point and minimum of the effective potential. In addition, at and below temperatures corresponding to $\beta\Delta\sim 10$, the anisotropy ratio of diffusion D_{yy}/D_{xx} tends towards a universal limit

$$\frac{D_{yy}}{D_{xx}}=\cot^2\theta , \tag{3.5}$$

which, for the W(110) surface, is two. This is *precisely* the value obtained using the simple random-walk theory in which atoms execute a random walk between the long bridge sites L.[6,7] An anisotropy ratio of two has also been experimentally measured for the O/W(110) system.[6] However, as our calculations demonstrate, the anisotropy ratio is very sensitive to temperature corrections of the diffusion prefactors *in addition to* the barrier, and thus the geometric limit generally appears at temperatures much lower than the beginning of the activated regime.

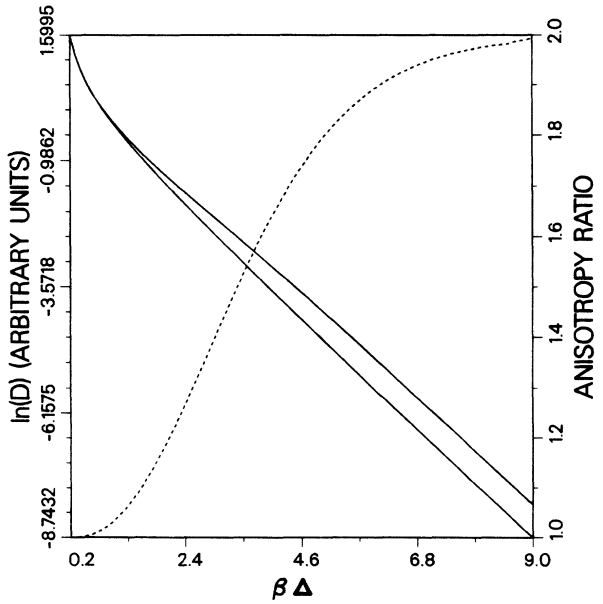

FIG. 3. D_{xx} (lower solid curve) and D_{yy} (upper solid curve) vs $\beta\Delta$ for the centered rectangular lattice of Fig. 2, using a simple cosine potential. The dashed line denotes the anisotropy ratio D_{yy}/D_{xx}, which tends to the universal value $\cot^2\theta=2$.

Another model potential, which we have used in our numerical calculations, is a temperature-dependent form given by

$$V_A(\mathbf{r})=\frac{1}{\beta}\ln\left[\sum_l (e^{-\beta\alpha_x(x-R^0_{l,x})^2}+e^{-\beta\alpha_y(y-R^0_{l,y})^2})\right] . \tag{3.6}$$

In Figs. 4(a) and 4(b), we show this potential at two different temperatures, with $\alpha_x=12$, $\alpha_y=4$. Figure 4(c) shows calculations of $\mathbf{D}$ for this potential using the same Debye-Waller factors as above and a friction tensor $\eta^{xx}=\eta^{yy}=1$, $\eta^{xy}=\eta^{yx}=0$. Again, this result recovers both the correct Arrhenius form, with an asymptotically temperature-independent energy barrier $\Delta=1$, and the universal ratio (3.5) at the limit of low temperatures. For this potential the anisotropy ratio approaches its low-temperature limit very fast due to a strong temperature dependence of the curvature around the saddle point, see Fig. 4(b). Our further calculations varying the adiabatic potentials and including spatial dependence in the friction tensor[13] always reproduce the universal low-temperature behavior. However, we note that the detailed form of $\mathbf{D}$ at intermediate temperatures is model dependent.

To verify the universal nature of the geometric result (3.5), we have done additional calculations using the geometry of Fig. 2, with $\theta=30°$. This corresponds to a slightly different rhomboidal lattice. We have again performed numerical calculations using a simple cosine potential. In Fig. 5 we show results for $\mathbf{D}$ using the friction tensor $\eta^{xx}=\eta^{yy}=\frac{1}{2}$, $\eta^{xy}=\eta^{yx}=0$. The Debye-Waller correction was the same as for the centered rectangular lattice. The results are also very similar, except that now the ratio D_{yy}/D_x tends to $\cot^2\theta=3$ for this geometry.

C. The simple rectangular lattice

The simplest case in which the possibility of physically different saddle points arises naturally, is the simple rectangular lattice. Using our analytic formula (2.36) and the potential

$$V_1(\mathbf{r})=V_A\cos(\mathbf{G}_{10}\cdot\mathbf{r})+V_B\cos(\mathbf{G}_{01}\cdot\mathbf{r}) , \tag{3.7}$$

where $V_A\neq V_B$ generates two distinct saddle points along

the x and y axes, we obtain a generalization of the square lattice solution (3.2) as

$$D_{xx}=\frac{1}{M\beta\eta^{xx}}[I_0(\beta V_A)]^{-2}\,,$$
$$D_{yy}=\frac{1}{M\beta\eta^{yy}}[I_0(\beta V_B)]^{-2}\,. \tag{3.8}$$

Both of these solutions start from their respective Brownian forms $D_{\alpha\alpha}=(k_BT)/M\eta^{\alpha\alpha}$ at high temperatures, and cross over to the Arrhenius form (AF) at low temperatures. However, the ratio D_{yy}/D_{xx} will go to zero exponentially fast for $V_B > V_A$, i.e., the saddle point with the lower energy barrier will dominate diffusion at low temperatures. In Fig. 6 we display a numerical solution of **D** for potential (3.7), with $\eta^{xx}=\eta^{yy}=1$, using Debye-Waller correction factors with the same parameters as for the centered rectangular lattice case.

There exists a recent experimental study of a surface with simple rectangular symmetry, and two distinct ener-

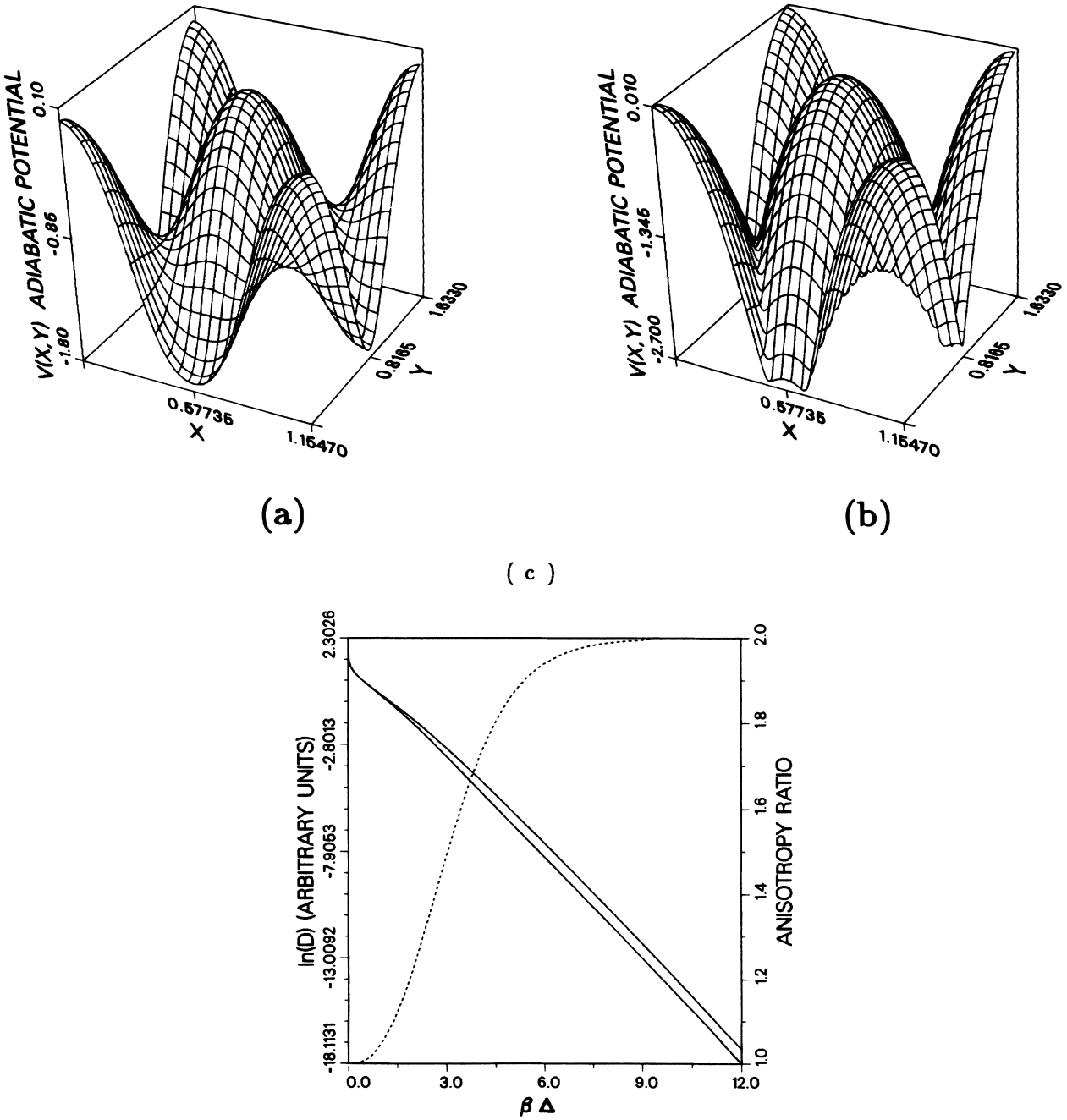

FIG. 4. (a) and (b) Temperature-dependent model potential (3.6) at (a) $\beta=1$ and (b) $\beta=8$. At low temperatures, a narrow ridge develops connecting the minima. (c) Results of D_{xx} (lower solid curve) and D_{yy} (upper solid curve) vs $\beta\Delta$ for the potential in (a) and (b). The dashed line is the anisotropy ratio D_{yy}/D_{xx}, which now approaches $\cot^2\theta=2$ rather rapidly.

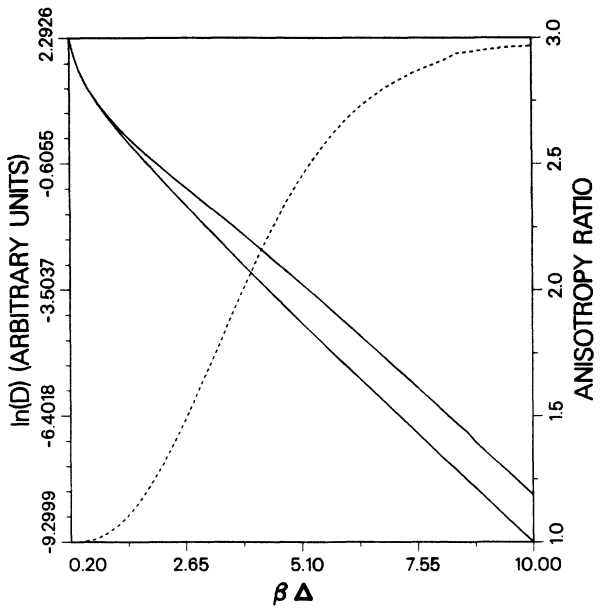

FIG. 5. D_{xx} (lower solid curve) and D_{yy} (upper solid curve) vs $\beta\Delta$ for the rhomboidal lattice of Fig. 2, with $\cot\theta=\sqrt{3}$. The dashed line denotes the anisotropy ratio D_{yy}/D_{xx} which tends to the universal value $\cot^2\theta=3$ for this case.

gy barriers.[17] This involves the self-diffusion of Tungsten on a clean W(211) surface. In Fig. 7(a), we show the experimentally measured components of the diffusion tensor. To illustrate the applicability of the microscopic theory presented here, we have done model calculations for this system. Using model potential of the form (3.7), we can incorporate the two different energy barriers seen in the experiments into the calculations. To obtain a quantitative fit, we have set the energy barriers $\Delta_x=1$, $\Delta_y=2.13$ (in normalized units, in which $\Delta_x=3125$ K), and used a constant anisotropic friction tensor with $\eta^{xx}/\eta^{yy}=0.0064$, $\eta^{xy}=\eta^{yx}=0$. Setting the absolute values of η^{xx} and η^{yy} will then determine **D** in real units corresponding to the experiments. Additionally, the Debye-Waller parameters were set to correspond to $\theta_D=240$ K, and the corresponding energy barriers for each spatial direction. In Fig. 7(b), we display the results of these model calculations which match with the experimentally observed curves very well. However, at higher

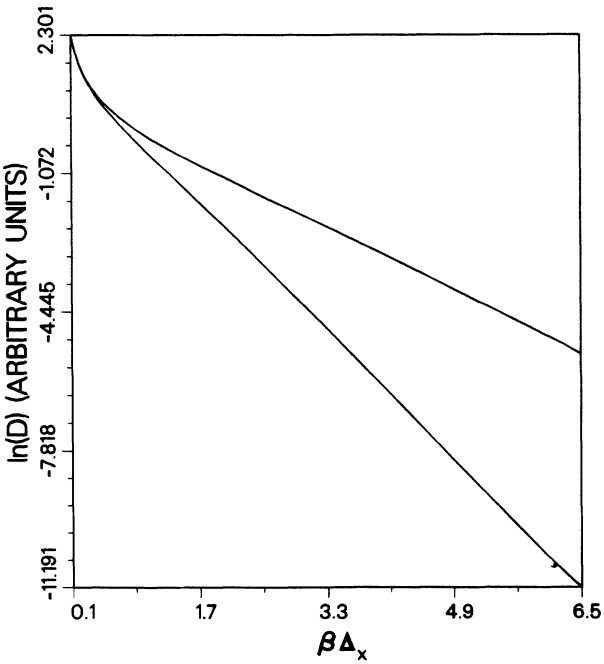

FIG. 6. Numerical solution for D_{xx} (upper curve) and D_{yy} (lower curve) vs $\beta\Delta_x$ for a simple rectangular lattice. Without the Debye-Waller correction factors, these curves can be obtained from the analytic result (3.8).

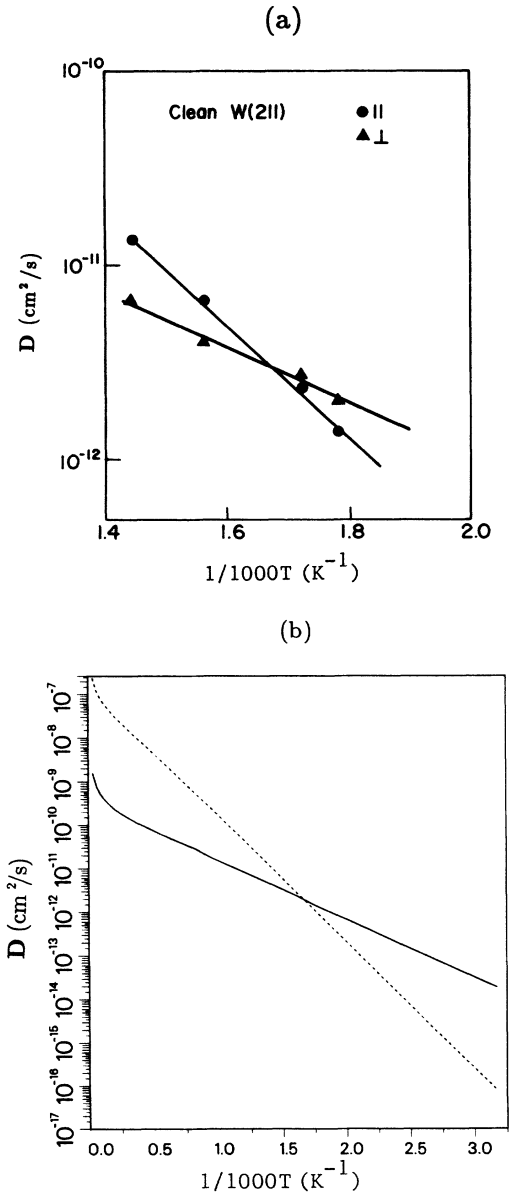

FIG. 7. (a) Experimental results of Tringides and Gomer (Ref. 17) for self-diffusion on the W(211) surface along two orthogonal directions. (b) Results of model calculations of W diffusion based on a simple rectangular lattice, as described in the text. D_{xx} (solid line) corresponds to the direction with the smaller barrier $\Delta_x=3125$ K.

temperatures we expect the simplified model used here not to be quantitatively correct.[18]

IV. DISCUSSION AND SUMMARY

The microscopic theory we have presented in this paper allows a systematic and well-controlled theoretical study of surface diffusion. By extending the previous theory[2] to include motion in the direction normal to the surface, we have developed a complete picture of classical adatom diffusion. We make *no assumptions* about activated diffusion jumps or particular diffusion trajectories, but express the diffusion tensor in terms of an inverse friction expansion. The present paper studies the high-friction limit, in which we present results at all temperatures. Even in the high-temperature limit, the theory recovers the universal Brownian motion result. Answers to the two fundamental questions we have addressed in this work, namely the emergence of the Arrhenius form of activated temperature dependence and the applicability of simple geometric random-walk picture, emerge in a natural way from the theory in the high-friction limit. In the low-temperature limit we always recover the Arrhenius form corresponding to the classical saddle-point barrier. One of the nontrivial results obtained from our general approach is the relatively larger sensitivity of the geometric random-walk anisotropy to temperature. The geometric limit for the anisotropy ratio is usually approached only at temperatures much lower than where the Arrhenius form is already a very good approximation for the temperature dependence of $\mathbf{D}$.[19] Deviations from the geometric limit arise from gradual increase in diffusion paths which do not follow the exact TST trajectories. Eventually, at high temperatures, this contribution becomes large enough to cause deviations from the activated behavior, and a crossover to Brownian behavior. All these results are *universal* (within the high-friction limit) in the sense that neither small oscillations in the vertical direction nor the detailed form of the adiabatic potential or the friction tensor change this picture qualitatively. This is well demonstrated by the excellent agreement with experiments obtained with a simple model of W diffusion on a simple rectangular lattice of Sec. III.

The existing theory can also be used to compute general frequency-dependent correlation functions, which can be related to the vibrational properties of adatoms on surfaces. It is also relatively straightforward to continue the continued fraction expansion of Sec. II and study the correlation functions beyond the high-friction approximation, although much of the transparency of the analytic result (2.36) is lost. This will certainly influence the details of the crossover behavior in temperature, but is not expected to drastically change the universal properties of diffusion discussed here. Work in these directions is already in progress.

ACKNOWLEDGMENTS

This work was supported by a U.S. Office of Naval Research (ONR) grant.

APPENDIX

In this appendix we want to show that the spatial matrix elements of $\mathbf{F}\equiv\mathbf{b}_{10}a_0^{-1}(\omega)\mathbf{b}_{01}$ are given by (2.19). First, by definition,

$$\mathbf{a}_0^{-1}(\omega)=\frac{i}{\omega}\chi_{00} \tag{A1}$$

and

$$\mathbf{b}_{nm}=i\chi_{nn}^{-1}\mathbf{c}_{nm}\chi_{mm}^{-1}\ , \tag{A2}$$

where $\mathbf{c}_{nm}\equiv(\mathbf{A}_n,L\,\mathbf{A}_m)$. Using the definition of the slow variables and the identity

$$\frac{d\psi_j(u)}{du}=\sqrt{2j}\,\psi_{j-1}(u)\ ,$$

the spatial matrix elements of $\mathbf{c}_{nm}$ can be written as

$$\mathbf{c}_{10}^{\alpha}(\mathbf{G},\mathbf{G}';j,j')=G'_{\beta}\chi_{11}^{\alpha\beta}(\mathbf{G},\mathbf{G}';j,j') -i(2j')^{1/2}\chi_{11}^{\alpha z}(\mathbf{G},\mathbf{G}';j,j'-1)\ , \tag{A3}$$

and

$$\mathbf{c}_{01}^{\alpha}(\mathbf{G},\mathbf{G}';j,j')=G_{\beta}\chi_{11}^{\beta\alpha}(\mathbf{G},\mathbf{G}';j,j') +i\sqrt{2j}\,\chi_{11}^{z\alpha}(\mathbf{G},\mathbf{G}';j-1,j')\ . \tag{A4}$$

Using the result $\chi_{11}=(k_BT/M)\chi_{00}\delta_{\alpha\beta}$ from (2.17), we get

$$\mathbf{c}_{10}^{\alpha}(\mathbf{G},\mathbf{G}';j,j')=\frac{k_BT}{M}G'_{\alpha}\chi_{00}(\mathbf{G},\mathbf{G}';j,j')\ ,$$
$$\mathbf{c}_{10}^{z}(\mathbf{G},\mathbf{G}';j,j')=-i\frac{k_BT}{M}(2j')^{1/2}\chi_{00}(\mathbf{G},\mathbf{G}';j,j'-1) \tag{A5}$$

and

$$\mathbf{c}_{01}^{\alpha}(\mathbf{G},\mathbf{G}';j,j')=\frac{k_BT}{M}G_{\alpha}\chi_{00}(\mathbf{G},\mathbf{G}';j,j')\ ,$$
$$\mathbf{c}_{01}^{z}(\mathbf{G},\mathbf{G}';j,j')=i\frac{k_BT}{M}\sqrt{2j}\,\chi_{00}(\mathbf{G},\mathbf{G}';j-1,j')\ , \tag{A6}$$

for $\alpha=x,y$. The final result follows immediately by substituting these equations together with (A1) to the definition of $\mathbf{F}$.

---

*Permanent address: Department of Physics, Tampere University of Technology, Box 527, SF-33101 Tampere, Finland.

[1]For a general review of diffusion, see, e.g., *Diffusion in Crystalline Solids,* edited by G. E. Murch and A. S. Norwick (Academic, New York, 1984).

[2]S. C. Ying, Phys. Rev. B **44**, 7068 (1990).

[3]H. Mori, Prog. Theor. Phys. **34**, 399 (1965); D. Forster, *Hydrodynamic Fluctuations, Broken Symmetry, and Correlation Functions* (Benjamin, Reading, 1975).

[4]K. Haug, C. Wahnström, and H. Metiu, J. Chem. Phys. **90**, 540

(1989); Z. Zhang and H. Metiu (unpublished).
[5]See, e.g., A. A. Deckert, J. L. Brand, M. V. Arena, and S. M. George, Surf. Sci. **208**, 441 (1989); S. C. Wang and G. Erlich, *ibid.* **206**, 451 (1988).
[6]M. Tringides and R. Gomer, Surf. Sci. **155**, 254 (1985); **166**, 419 (1986).
[7]J. Kjoll, T. Ala-Nissila, and S. C. Ying, Surf. Sci. **218**, L476 (1989); J. Kjoll, T. Ala-Nissila, S. C. Ying, and R. Tahir-Kheli (unpublished).
[8]J. D. Doll and A. F. Voter, Annu. Rev. Phys. Chem. **38**, 413 (1987); A. F. Voter and J. D. Doll, J. Phys. Chem. **82**, 80 (1985); J. M. Cohen and A. F. Voter, J. Chem. Phys. **91**, 5082 (1989).
[9]J. C. Tully, G. H. Gilmer, and M. Schugard, J. Chem. Phys. **71**, 1630 (1979).
[10]S. Paik and S. Das Sarma, Surf. Sci. **208**, L53 (1989); J. D. Doll and H. K. McDowell, J. Chem. Phys. **77**, 479 (1982).
[11]C. P. Flynn and G. Jacucci, Phys. Rev. B **25**, 6225 (1982).
[12]T. Ala-Nissila and S. C. Ying, Phys. Rev. Lett. **65**, 879 (1990).
[13]G. Wahnström, Surf. Sci. **159**, 311 (1985).
[14]See G. Wahnström, Surf. Sci. **164**, 437 (1985), and references therein.
[15]W. Jones and N. H. March, *Theoretical Solid State Physics,* (Wiley, New York, 1973), Vol. I.
[16]M. S. Altman, P. J. Estrup, and I. K. Robinson, Phys. Rev. B **38**, 5211 (1988).
[17]M. Tringides and R. Gomer, J. Chem. Phys. **84**, 4049 (1986).
[18]D. -S. Choi and R. Gomer, Surf. Sci. **230**, 277 (1990).
[19]This behavior is even more pronounced for more complicated, locally distorted surface potentials [T. Ala-Nissila and S. C. Ying, Surf. Sci. Lett. **235**, 341 (1990)].